Spinal interleukin-17 promotes thermal hyperalgesia and NMDA NR1 phosphorylation in an inflammatory pain rat model

Xianze Meng[1,2,a], **Yu Zhang**[3,a], **Lixing Lao**[2], **Rikka Saito**[2], **Aihui Li**[2], **Cristina M. Bäckman**[4], **Brian M. Berman**[2], **Ke Ren**[5], **Pin-Kang Wei**[1], and **Rui-Xin Zhang**[2,*]

[1]Department of Traditional Chinese Medicine, Shanghai Changzheng Hospital, Second Military Medical University, Shanghai, 200001, P. R. China

[2]Center for Integrative Medicine, School of Medicine, University of Maryland, Baltimore, MD 21201 USA

[3]Department of Neurobiology, Shanxi Medical University, Taiyuan 030001, Shanxi, P. R. China

[4]Integrative Neuroscience Research Branch, National Institute on Drug Abuse, National Institutes of Health, Baltimore, MD 21224-6825 USA

[5]Department of Neural and Pain Sciences, Dental School, University of Maryland, Baltimore, MD 21201 USA

Abstract

It is known that interleukin-17 (IL-17) is associated with autoimmune disorders and that peripheral IL-17 plays a role in arthritis and neuropathic pain. The present study investigated the possibility of spinal cell expression of IL-17 during inflammatory pain and possible IL-17 involvement in such pain. Hyperalgesia was induced by injecting complete Freund's adjuvant (CFA, 0.08 ml, 40 μg *Mycobacterium tuberculosis*) into one hind paw of the rat. Paw withdrawal latency (PWL) was tested before (−48 h) and 2 and 24 h after CFA to assess hyperalgesia. IL-17 antibody (0.2–2 μg/rat) was given intrathecally (i.t.) 24 h before CFA to block the action of basal IL-17 and 2 h prior to each of two PWL tests to block CFA-induced IL-17. I.t. recombinant IL-17 (10–400 ng/rat) was administered to naive rats to determine its effects on PWL and phosphorylated-NR1 (p-NR1). P-NR1 modulates N-methyl-D-aspartate receptor (NMDAR) activity to facilitate pain. Spinal cords were removed for IL-17 immunostaining, double immunostaining of IL-17/cell markers and IL-17 receptor A (IL-17RA)/NR1, for western blot of IL-17, p-NR1, IL-17RA, and GFAP, for *in situ* IL-17RA hybridization, and for real time PCR of IL-17RA. The data shows that 1) IL-17 is up-regulated in activated and non-activated astrocytes, 2) IL-17RA is localized in NR1-immunoreactive neurons and up-regulated, and 3) IL-17 antibody at 2 μg/rat significantly increased PWL (P<0.05) and decreased p-NR1 and IL-17RA compared to control in CFA- and IL-17-injected rats. The results suggest that spinal IL-17 is produced by astrocytes and enhances p-NR1 to facilitate pain.

*Corresponding author: Dr. Rui-Xin Zhang, Center for Integrative Medicine, 685 W. Baltimore Street, MSTF Rm 8-22, Baltimore, MD 21201, Telephone: 410-706-1582, Fax: 410-706-1583, Rzhan001@umaryland.edu.
[a]They made equal contributions to this work.

The authors do not have any conflicts of interest.

Publisher's Disclaimer: This is a PDF file of an unedited manuscript that has been accepted for publication. As a service to our customers we are providing this early version of the manuscript. The manuscript will undergo copyediting, typesetting, and review of the resulting proof before it is published in its final citable form. Please note that during the production process errors may be discovered which could affect the content, and all legal disclaimers that apply to the journal pertain.

1. Introduction

The interleukin-17 (IL-17) cytokine family has recently emerged as a critical player in immune system and inflammatory diseases. The family consists of six ligands (IL-17A–F) and five receptors (IL-17RA–IL-17RE) in mammals [6]. IL-17A, also known as IL-17, the prototypical IL-17 ligand, is mainly produced by a subset of CD4(+) T helper (TH) cells now known as TH17 cells [29; 39]. These act on IL-17RA to up-regulate the expression of inflammatory genes such as IL-6, IL-8, granulocyte-colony-stimulating factor, and prostaglandin E2 in epithelial, endothelial, and fibroblastic cells [5]. It is well known that IL-17 is elevated in multiple sclerosis, rheumatoid arthritis, and psoriasis [11; 21] and is involved in these autoimmune disorders [18; 21; 30].

Recent studies have shown that glial cells of the central nervous system also express IL-17. For example, IL-17 was produced in the astrocytes of rats with permanent middle cerebral artery occlusion [17] and in brain astrocytes of patients with multiple sclerosis [33]. It is also well known that glial cells, including astrocytes and microglia, are activated in the lumbar spinal cord in inflammatory [25; 32; 37] and neuropathic pain models [20; 24; 31]. Glial cells release a variety of algesic substances, including proinflammatory cytokines such as IL-1β, TNF-α, and IL-6, which may potentiate transmission and processing of noxious inputs at the spinal level [25; 38]. Whether spinal glial cells produce IL-17 during inflammatory pain and whether IL-17 is involved in such pain have not been studied.

A few studies show involvement of peripheral IL-17 in pain. For example, IL-17 was detected in the injured nerves of neuropathic pain models [15; 22], and intra-hind paw [13; 19] and intra-knee [23] injections of recombinant IL-17 in mice induced hyperalgesia. Further, the concentration of IL-17 in the spinal cord of rats is increased after nerve injury [2]. IL-17 knockout (KO) mice displayed significantly decreased mechanical hypersensitivity compared to normal mice in a neuropathic pain model of partial ligation of the sciatic nerve [13], which suggests that central nervous system IL-17 might be involved in pain. In the present study, we sought to determine whether spinal cells express IL-17 after inflammation and whether IL-17 is involved in the inflammatory pain. We also investigated whether IL-17 modulates the phosphorylation of NR1, an essential subunit of the N-methyl D-aspartate receptor (NMDAR) that is known to modulate NMDAR activity and facilitate nociceptive input transmission in inflammatory pain models [7; 44; 45].

2. Methods

2.1. Animal Preparation

Male Sprague-Dawley rats weighing 270–300 g (Harlan, Indianapolis, IN) were kept under controlled laboratory conditions (22°C, relative humidity 40%–60%, 12-h alternate light–dark cycles, food and water *ad libitum*) and were acclimatized to the environment for five days prior to experimentation. The animal protocols were approved by the Institutional Animal Care and Use Committee (IACUC) of the University of Maryland School of Medicine, Maryland, USA.

2.2. Experimental Design

Five sets of experiments were conducted to determine spinal IL-17 involvement in hyperalgesia: 1) immunostaining to show IL-17-immunopositive cells and IL-17RA/

NMDAR NR1 co-localization, 2) Reverse transcription polymerase chain reaction (RT-PCR) and in situ hybridization to determine IL-17 and IL-17RA mRNA expression, 3) complete Freund's adjuvant (CFA)- or saline-injected rats plus IL-17 antiserum, 4) naive rats plus IL-17 protein, and 5) western blot to examine IL-17RA, IL-17, GFAP and NMDAR NR1 phosphorylation levels in the spinal cord.

In experiment 1, double immunofluorescence was used to identify the cell type that produces IL-17 during inflammatory pain and IL-17RA/NMDA NR1 co-localization. In sub-experiment 1, CFA-inflamed rats were randomly divided into 2 h and 24 h post-CFA injection groups (n=3 per group). Another 3 rats, 24 h post-saline injection, were used as control. The lumbar spinal cord was used for IL-17 immunostaining and double immunofluorescence staining of IL-17 with glial fibrillary acidic protein (GFAP), OX-42, and NeuN, the respective markers of astrocytes, microglia, and neurons. In sub- experiment 2, spinal cord sections from the 24 h group were double stained for IL-17RA and NR1 to determine whether IL-17RA is localized in NMDAR-containing neurons. In sub-experiment 3 (n=3 per group), spinal cord sections from the 24 h post-CFA rats were stained for ROR gamma, a molecular marker for TH-17 lymphocytes, and CD14, a monocyte marker. These two types of cells are known to produce IL-17 and to infiltrate the brain parenchyma in the experimental autoimmune encephalomyelitis (EAE) rat model [1]. The mesenteric lymph nodes were used as a positive control.

In experiment 2, RT-PCR, real time PCR and in situ hybridization were performed in two groups of rats (n=2–6 per group) to determine whether the spinal cord expresses IL-17 and IL-17RA mRNA. The IL-17RA mRNA were quantified with real time PCR (n=6 per group).

In experiment 3, antiserum against IL-17 was administered to CFA- or saline-injected rats to determine whether it alleviates pain. CFA or saline was subcutaneously injected into the plantar surface of one hind paw. The CFA-injected rats were randomly divided (n=7 per group) into a control group and two IL-17 antiserum (Cat# sc-7927, Santa Cruz Biotechnology, Inc) groups, 0.2 and 2 μg/rat (10 μl). I.t. IL-17 antiserum was given three times, 24 h before CFA to block the action of basal IL-17 and 2 h prior to each of two hyperalgesia tests, to block CFA-induced IL-17. The control group received saline (10 μl, i.t.) on the same schedule. Three sub-groups of the saline-injected rats were similarly treated. Paw withdrawal latency (PWL) tests were conducted before CFA (−48 h) for baseline and 2 and 24 h after CFA to measure thermal hyperalgesia.

In experiment 4, naive rats were divided into five groups (n=7 per group), which were respectively treated with saline, IL-17 at 10 ng, 100 ng, and 400 ng/rat, and IL-17 at 400 ng/rat plus 2 μg of antiserum against IL-17. IL-17 protein (ProSpec-Tany TechnoGene Ltd) was dissolved in saline and injected i.t. into the lumbar spinal cord. PWL was measured −48 h prior to and 2, 24, and 48 h after the injection.

In experiment 5, since IL-17 induced the most significant decrease of PWL 24 h after the IL-17 injection, the spinal cord was removed at that time point in five groups (n=4 per group) of rats treated as in experiment 4. The spinal cords were also removed from rats of experiment 3 after PWL testing 24 h post-CFA injection and from another group of rats 2 h post-CFA injection. Relative levels of IL-17RA, NR1 phosphorylation, IL-17, and GFAP were measured with western blot.

2.3. I.t. drug delivery

Lumbar punctures were performed as previously described [16]. A PE10 polyethylene tube (Clay Adams) was submerged in 70°C water, stretched to about 150% of its original length to reduce the diameter, and used as an injection catheter. With a 29-gauge needle, another

10-cm PE10 tube was connected to one end of the catheter and then to a 50-µl glass Hamilton syringe with a PE50 tube. The injection catheter was prefilled with 10 µl of drug or vehicle separated from 5 µl of saline by a small air bubble. Under isoflurane anesthesia, the dorsal pelvic area was shaved and swabbed with 70% alcohol. A 21-gauge sterile needle with the plastic hub removed was inserted between lumbar vertebrae L5 and L6. The catheter was inserted into the guide needle and rostrally advanced 4 cm from the tip of the needle into the lumber enlargement, where its arrival was confirmed by a tail-twitch. The drug, or vehicle, was injected and followed by a saline flush. Three minutes after the injection the catheter was withdrawn and the needle was removed from the intervertebral space.

2.4. Induction of hyperalgesia

Inflammatory hyperalgesia was induced by injecting CFA (Sigma, St Louis, MO; 0.08 ml, 40 µg *Mycobacterium tuberculosis*), suspended in an 1:1 oil/saline emulsion, subcutaneously into the plantar surface of one hind paw of the rat using a 25-gauge hypodermic needle [41]. The inflammation, manifesting as redness, edema, and hyper-responsiveness to noxious stimuli, was limited to the injected paw and appeared shortly after the injection. Hyperalgesia was determined by a decrease in PWL to a noxious thermal stimulus.

2.5. Thermal hyperalgesia

The rats in experiments 3 and 4 were tested for PWL by a previously described method [9; 41]. They were placed under an inverted clear plastic chamber on the glass surface of a Paw Thermal Stimulator System (UCSD, San Diego) and allowed to acclimatize for 30 min before the test. A radiant heat stimulus was applied with a projector lamp bulb (CXL/CXR, 8 V, 50 W) to the plantar surface of each hind paw from underneath the glass floor. PWL to the nearest 0.1 s was automatically recorded when the rat withdrew its paw from the stimulus. Stimulus intensity was adjusted to derive an average baseline PWL of approximately 10.0 s in naive animals. Paws were alternated randomly to preclude "order" effects. A 20-s cut-off was used to prevent tissue damage.

Mean PWL was established by averaging the latency of four tests with a 5-min interval between each test. The investigator who performed the behavioral tests was blind to group assignment.

2.6. Immunofluorescence

Rats were deeply anesthetized with sodium pentobarbital (60 mg/kg, i.p.) and immediately perfused transcardially with 4% paraformaldehyde (Sigma) in 0.1 M phosphate buffer (PB) at pH 7.4. The lumbar 4–5 spinal cord was removed, immersed in the same fixative for 2 h at 4 °C, and transferred to 30% sucrose (w/v) in PB saline (PBS) overnight for cryoprotection. Thirty micron-thick sections were cut on a cryostat, rinsed in PBS, blocked in PBS with 10% normal donkey serum for 60 min, and incubated overnight at room temperature with a mixture of rabbit polyclonal antibody against IL-17 (1:50, Cat# sc-7927, Santa Cruz Biotechnology, Inc) and mouse monoclonal antibodies against GFAP (1:500, Chemicon), OX-42 (1:500, Biosource) or NeuN (1:500, Chemicon). After three 10-min washings in PBS, sections were incubated in a mixture of CY2-conjugated donkey anti-rabbit (1:200, Jackson ImmunoResearch Laboratories) and CY3-conjugated donkey anti-mouse (1:500) for 1 h at room temperature. Control sections were similarly processed, except that the primary antisera were omitted. The stained sections were mounted on gelatin-coated slides, coverslipped with aqueous mounting medium (Biomeda Corp., CA), and examined under a Nikon fluorescence microscope. IL-17 immunostained cells were magnified with a 20× objective lens and counted in 10 randomly-selected sections from each

rat. The results were averaged for each individual rat and then for the group. Double labeling of IL-17RA (1:50, Cat# sc-30175, Santa Cruz) and NR1 (1:500, Santa Cruz Biotechnology) was performed the same way. ROR gamma (1:2000, Abcam) and CD 14 (1:2000, Santa Cruz) immunostaining were performed according to the standard ABC method.

2.7. *In situ* hybridization

Rats (n=3) were perfused with 4% formaldehyde in 0.1M PBS. Spinal cord samples were post-fixed in the same fixative for 24 h at 4°C, dehydrated, and embedded in paraffin. For the IL-17RA gene (gene bank #NM_001107883.2), a set of 20 specific probes (25 bp in length on average) that span a ~1 kb region of IL-17RA mRNA were synthesized. Spinal cord sections, 5 μm in thickness, were used for *in situ* hybridization with RNAscope (Advanced Cell Diagnostics) following the manufacturer's protocol [36]. Briefly, the deparaffinized sections were pretreated with heat and protease before hybridization with the target probes for 2 h at 40°C. A horseradish peroxidase-based signal amplification system was hybridized to the target probes followed by color development with 3,3-diaminobenzidine and counterstaining with Gill's Hematoxylin. The stained sections were coverslipped with DPX (Electron Microscopy Science) and examined under a Nikon microscope. Positive staining was identified as brown, punctate dots present in the cytoplasm. We used a positive control, RNAscope Positive Control Probe, POLR2A (Advanced Cell Diagnostics, cat# 312481), and a negative one, RNAscope Negative Control Probe, DapB (Advanced Cell Diagnostics, cat# 310043), on spinal cord tissue.

2.8. RT-PCR for IL-17 and real time PCR for IL-17RA

Rats (n=2–6) were anesthetized with isoflurane and decapitated. The spinal cord was removed. The dorsal horn was separated into ipsilateral and contralateral sections and stored immediately in dry ice; mesenteric lymph nodes were removed for IL-17 positive control. Total RNA was extracted with Ambion RNAqueous® Kit according to the manufacturer's protocol. The RNA sample was treated with RNase-free DNase I (Ambion 2224G1). An Invitrogen Reverse Transcriptase Kit was employed to generate the cDNA. For IL-17, the forward and reverse primers are 5′-gaagttggaccaccacatga-3′ and 5′-tccctcttcaggaccaggat-3′; for IL-17RA, they are 5′-gacccaaaccacaagtccaa-3′ and 5′-gtcatcttcatctccgtgtcc-3′; for house keeping gene, hydroxymethylbilane synthase (Hmbs), they are 5′-tccctgaaggatgtgcctac-3′ and 5′-acaagggtttttcccgtttg-3′; for house keeping gene, hypoxanthine phosphoribosyltransferase minigenes (Hprt), they are 5′-ggtccattcctatgactgtagatttt-3′ and 5′-caatcaagacgttctttccagtt-3′. Primers were reconstituted to a final concentration of 30 μM and were mixed according to the Qiagen protocols so that each well of an ABI 96 well optical reaction plate (Applied Biosystems, USA) contained 10x buffer 2 μl, 10 mM dNTP 1μl, 0.2 μl of Roche rat universal probe, 1μl of the primer pair solution, 25 mM MgCl$_2$ 2.8 μl, and either 10 μl cDNA for spinal cord IL-17, 2 μl of cDNA for mesenteric lymph nodes IL-17, or 2 μl cDNA for spinal cord IL-17RA. H$_2$O was added for a total reaction volume of 20 μl. The plate was loaded into an 7900HT real time PCR System (Applied Biosystems, USA) at 95° C for 2 min followed by 50 cycles of 95° C for 15 s, 60 °C for 30 s, and 72° C for 30 s. The PCR products of IL-17 were electrophoresed on 2% agarose gel and photographed. The relative levels of IL-17RA were normalized to internal controls Hmbs, and Hprt. The standard curve method was used to compare mRNA expression levels between groups. Normalization to both endogenous control genes led to similar results.

2.9. Western blot

Western blot was used to examine phosphorylated NR1 (p-NR1), IL-17RA, IL-17, and GFAP. The rats in experiments 3 and 5 were anesthetized with sodium pentobarbital (60 mg/kg, i.p.) and decapitated 2 and 24 h post-CFA or -IL-17 respectively. The spinal cord was

removed with a high-pressure injection of saline into the sacral spinal cord and the ipsilateral and contralateral dorsal divisions of the lumbar 4–5 spinal cord were harvested. The ipsilateral and contralateral portion of the spinal cord dorsal horn was homogenized in protein extraction buffer containing 1% EDTA and 1% Halt™ Protease and Phosphatase Inhibitor Cocktail (Thermo scientific) and centrifuged at 14000 rpm for 10 min at 4°C, after which the supernatant containing the proteins was collected. Protein concentration was determined using the Bio-Rad Protein Assay. Equal amounts of protein were mixed with loading buffer. After heating in 95° C for 10 min, the proteins were fractionated on a 4–20% (w/v) SDS-PAGE and transferred onto a polyvinylidine difluoride (PVDF) membrane (Bio-Rad) with a Trans-Blot Cell System (Bio-Rad). The membrane was blocked for 1 h at room temperature with 5% milk in TBS (20 mM Tris, 150 mM NaCl, pH 7.4) containing 0.1% Tween 20 (TBST) and then incubated overnight at 4°C with phosphor-NR1 antiserum (Serine 896, 1:500, Cat# sc-31669-R, Santa Cruz) or IL-17RA antiserum (1:500, Cat# sc-30175, Santa Cruz), IL-17 (1:200, Cat# sc-7927, Santa Cruz), or GFAP antiserum (1:5000, Chemicon). Membranes were washed with TBST buffer and incubated for 2 h at room temperature with goat anti-rabbit horseradish peroxidase-conjugated IgG (1:2000; KPL) diluted in 5% (w/v) milk in TBST buffer. The immunoreactivity of the proteins on the membrane was visualized using the enhanced chemilluminescence detection system (ECL, Thermo scientific). Autoradiograms were digitized, and densitometric quantification of immunoreactive bands was carried out using Scion NIH Image 1.60. The membranes were then incubated in stripping buffer (Thermo scientific) at room temperature for 20 min and re-probed with β-actin antibody (1:5000, Sigma) as a loading control. Those who harvested the tissue and performed the western blot were blinded to the treatment.

2.10. Statistical analyses

Data from the thermal hyperalgesia tests were presented in Mean ± S.E.M. and analyzed using repeated measures analysis of variance (ANOVA) followed by Scheffé's multiple comparisons (Statistical Analysis System). Western blot data and immunostaining data were analyzed with one-way between-subject ANOVA followed by the Scheffé's multiple comparison. Real time PCR data were analyzed with one-way ANOVA followed by Bonferroni's multiple comparison. $P<0.05$ was set as the level of statistical significance.

3. Results

3.1. IL-17 localization in the spinal cord

Double immunofluorescence labeling demonstrated that IL-17 immunoreactivity was co-localized with the astrocyte marker GFAP but not with the microglia marker OX-42 or the neuronal marker NeuN (Fig. 1). IL-17-labeled glial cells were localized in laminae I–II, III–IV, V–VI and X. In laminae I–II, the number of ipsilateral IL-17 immunoreactive cells 2 and 24 h post-CFA was significantly increased compared to that in saline control rats (P<0.05). The number of contralateral IL-17 immunoreactive cells was slightly but not significantly higher than that in saline control rats. The number of ipsilateral IL-17 immunoreactive cells was also significantly higher than that of contralateral IL-17 immunoreactive cells 24 h post CFA (P<0.05). See Fig. 2.

In laminae V–VI, IL-17 immunoreactive cells were significantly increased both ipsilaterally and contralaterally 2 h post-CFA compared to those of saline control rats, as were ipsilateral cells 24 h post-CFA. In lamina X, IL-17 was significantly elevated 2 h but not 24 h post-CFA compared to that in saline control rats. In laminae III–IV, no significant differences were observed. This implies that IL-17 was up-regulated in astrocytes between 2 and 24 h after inflammation was produced. Control sections without primary antibodies showed no specific staining.

It was found that some astrocytes exhibited hypertrophy with larger and more densely stained cell bodies after inflammation (Fig. 1a***). As shown in Fig. 1 a***, IL-17 was produced in both activated and non-activated astrocytes. Western blot showed significant GFAP up-regulation in the ipsilateral spinal dorsal horn 2–24 h post-CFA compared to saline control (Fig. 3).

To investigate the possibility that IL-17 was expressed by TH-17 lymphocyte and monocyte infiltration into the spinal cord, we immunostained for ROR gamma and CD14. The results showed strong ROR gamma and CD14 staining in the mesenteric lymph nodes but not in the spinal cord ipsilateral to CFA injection (Supplemental Fig. 1). The data indicate that the IL-17 mRNA expressed in the spinal cord in our experiments is from astrocytes and not from either TH-17 lymphocytes or monocytes.

3.2. IL-17 mRNA RT-PCR and IL-17RA mRNA real time PCR and in situ hybridization

It was noted that spinal cord cDNA has to be used at 5 times the positive control (mesenteric lymph node cDNA) to get the RT-PCR product for IL-17, showing amplification after 30–35 cycles, which are not suitable for quantification of IL-17 mRNA with real time PCR. The RT-PCR results show that IL-17 mRNA was expressed in the dorsal horn of the spinal cord (Fig. 4). Regarding the gel, the bands represent the total PCR product after 50 cycles of amplification. As a saturation effect detected by ethidium bromide at that level of 50 cycles of amplification, we do not see differences among the bands. Thus, we do not know whether the initial quantity of available IL17 mRNAs are similar between groups.

The real time PCR showed that relative levels of IL-17RA mRNA were not significantly different in the dorsal horn of the spinal cord among three groups of rats, saline 24 hr, CFA 2 hr and CFA 24 hr (Fig. 5).

The *in situ* hybridization data show that IL-17RA mRNA is expressed in oval and round cells at ~ 7μm (Fig. 6). Most of those IL17RA mRNA-positive cells in the spinal cord looks to be neurons, although other cells such as T-lymphocytes, microglia and astrocytes may express IL17RA. Given that there is no positive T cell staining in the spinal cord ipsilateral to CFA injection (Supplemental Fig. 1) and that there is large degree of overlap between IL17RA and NR1 protein staining in the spinal cord ipsilateral to CFA injection (Fig 7), we believe the vast majority of IL17RA protein is expressed by neurons.

As indicated above, the level of IL17 mRNA is quite low in the spinal dorsal horn. Therefore, we could not obtain positive IL-17 mRNA staining with RNAscope in situ hybridization technique (data not shown). This suggests that the RNAscope in situ hybridization is not sensitive enough to label the mRNA that has quite lower levels, whose detection needs more cDNA during RT-PCR than the standard method.

3.3. Co-localization of NR1 and IL-17RA

Double immunofluorescence labeling demonstrated that NR1 and IL-17RA co-localize in neurons of spinal cord ipsilateral to CFA injection. As shown in Fig. 7, IL-17RA immunoreactivity is completely localized in NR1-immunoreactive neurons in the spinal cord.

3.4. IL-17 antiserum alleviated hyperalgesia

Before CFA, the overall mean baseline PWL to noxious heat stimuli was similar in all groups of rats, and there was no significant difference between left and right PWL. After a 0.08 ml injection of CFA into the left hind paw, PWL of that paw was significantly shorter

than that of the contralateral hind paw, which was unchanged from baseline (Fig. 8A). Saline injection into the hind paw produced no changes in PWL (Fig. 8B).

In CFA-injected rats, IL-17 antiserum pretreatment dosage-dependently alleviated the CFA-induced hyperalgesia assessed by the PWL test. A 2 (ipsilateral, contralateral) $\times$ 3 (saline, 0.2, and 2 μg IL-17 antiserum) $\times$ 3 (baseline, 2, and 24 h) repeated-measures ANOVA revealed the main effect of drug treatment ($F_{(2, 18)} = 3.96$, p <0.05), time ($F_{(2, 98)} = 22.99$, P<0.001), side ($F_{(1, 98)} = 99.71$, P<0.001), and the interaction of drug treatment and time ($F_{(4, 98)} = 0.34$, p= 0.84). *Post hoc* means comparisons revealed that i.t. IL-17 antiserum at 2 μg/rat significantly increased PWL compared to saline treatment (P<0.05). Contralateral PWL did not change after the IL-17 antiserum treatment in CFA-injected rats (Fig. 8A), nor did PWL in saline-injected rats (Fig. 8B). The results indicate that IL-17 antiserum alleviates inflammation-induced hyperalgesia but does not affect nociception in an uninflamed hind paw.

3.5. IL-17-protein induced hyperalgesia

IL-17 dosage-dependently induced a significant decrease in PWL of both hind paws. At 10 ng, the PWL did not show any significant changes. At 100–400 ng, the decrease began 2 h and peaked 24 h after administration; PWL normalized 48 h after the injection (Fig. 9). Repeated-measures ANOVA revealed the main effect of drug treatment ($F_{(4,31)} = 7.38$, p <0.001), time ($F_{(3,91)} = 15.04$, P<0.0001), and the interaction of drug treatment and time ($F_{(11, 91)} = 2.37$, p< 0.05). *Post hoc* means comparisons revealed that i.t. IL-17 at 100 ng and 400 ng/rat significantly decreased PWL compared to saline control (P<0.01 and P<0.0001, respectively). IL-17 plus its antiserum in naive rats did not differ from saline control. The analytical results indicate that IL-17 at 100–400 ng/rat induces hyperalgesia that diminishes 48 h post- injection and that IL-17 antiserum pretreatment significantly blocks IL-17-induced decrease of PWL (Fig. 9).

3.6. IL-17RA, p-NR1 and IL-17 expression during CFA-induced pain

As shown in Fig. 10, IL-17RA, p-NR1, and IL-17 were significantly (P<0.05) higher in the ipsilateral spinal dorsal horn of CFA-injected rats 2–24 h after a CFA injection than in the contralateral spinal dorsal horn. These values were also significantly higher in CFA-injected than saline-injected rats, showing that CFA enhanced IL-17RA and IL-17 expression and NR1 phosphorylation.

3.7. IL-17 antiserum inhibited CFA- and IL-17-induced NR1 phosphorylation and IL-17RA up-regulation in the spinal cord

Fig. 11A shows the effects of IL-17 antiserum treatment on NR1 phosphorylation in the spinal cord. P-NR1 levels were significantly higher in vehicle-treated CFA rats than in saline-injected control. The levels were significantly lower in CFA-injected rats given 2 μg IL-17 antiserum than in rats given vehicle (P<0.05). This suggests that IL-17 antiserum inhibits spinal cord NR1 phosphorylation during peripheral hind paw inflammation. Fig. 11B shows the effect of IL-17 on p-NR1 in the spinal cord of naive rats. IL-17 dosage-dependently induced NR1 phosphorylation, paralleling the behavioral hyperalgesia induced by i.t. IL-17. IL-17 antiserum pretreatment significantly blocked IL-17-induced p-NR1. These data suggest that up-regulated endogenous IL-17 facilitates spinal cord NR1 phosphorylation to promote hyperalgesia.

Fig. 12A shows the effects of IL-17 antiserum treatment on IL-17RA in the spinal cord. IL-17RA levels were significantly higher in CFA-injected rats than in saline-injected control rats (P<0.05) and significantly lower in rats given 2 μg IL-17 antiserum than in rats given

vehicle or 0.2 μg IL-17 antiserum (P<0.05). This suggests that IL-17 antiserum inhibited CFA-induced IL-17RA up-regulation.

Fig. 12B shows the effect of IL-17 on IL-17RA in the spinal cord of naive rats. IL-17 dosage-dependently increased IL-17RA. IL-17 antiserum pretreatment significantly blocked such up-regulation. These data suggest that endogenous IL-17 facilitated expression of IL-17RA to promote hyperalgesia.

4. Discussion

4.1. IL-17 is up-regulated in astrocytes in the spinal dorsal horn

The present study demonstrates that IL-17 increases significantly in the ipsilateral spinal cord dorsal horn during CFA-induced inflammatory pain. Further, double immunostaining demonstrated that IL-17 is selectively produced in activated and non-activated astrocytes but not in microglia or neurons. Paralleling the finding that astrocytes exhibit hypertrophy in the spinal cord, western blot showed that GFAP was significantly up-regulated in the ipsilateral spinal dorsal horn. These data are consistent with our previous report that a CFA injection into the masseter of the rat induced significant GFAP up-regulation in spinal trigeminal nuclei 0.5 h-7 d post-CFA injection [8]. Our RT-PCR experiment shows that the spinal cord expresses IL-17 mRNA, and immunostaining data confirm that TH-17 lymphocytes and monocytes, cells known to produce IL-17 and to infiltrate the brain parenchyma in the EAE rat model [1], were not present in the spinal cord 24 h post-CFA injection. These data suggest that spinal cord astrocytes express IL-17 mRNA and IL-17. This is consistent with previous studies demonstrating that IL-17 was produced in astrocytes in rats with permanent middle cerebral artery occlusion [17] and in patients with multiple sclerosis [33]. It is noted that IL-17 mRNA level is much lower in the spinal cord since the RT-PCR product only appeared after 30–35 cycles, which are not suitable for quantification of IL-17 mRNA with real time PCR. Thus, we do not know whether there was an up-regulation of IL-17 mRNA during CFA-induced pain. It is likely that the IL-17 up-regulation is due to the enhanced translation.

The data suggest that astrocytes release IL-17 during pain. Since IL-17 exhibits proinflammatory activities similar to those of innate immune cytokines such as IL-1 β [6], which is up-regulated in the spinal cord during inflammatory pain [25; 28; 32; 38; 42], the IL-17 released in the spinal cord might be involved in inflammatory pain.

4.2. IL-17 antiserum attenuates inflammatory hyperalgesia

Another main finding of the present study is that i.t. IL-17 antiserum attenuates inflammatory hyperalgesia. This indicates that endogenous spinal IL-17 promotes transmission of noxious messages. In support of this, i.t. IL-17 protein significantly induced a decrease of PWL, which was antagonized by co-treatment with IL-17 antiserum. These data demonstrate that spinal IL-17 facilitates inflammatory pain. This is consistent with a prior study in a mouse neuropathic pain model of partial ligation of the sciatic nerve in which i.t. IL-17 produced thermal hyperalgesia and IL-17 KO mice displayed significantly decreased microglia and astrocyte activation in the L3–5 spinal cord plus decreased mechanical pain hypersensitivity [13]. These data suggest that during both inflammatory and neuropathic pain, spinal IL-17 is involved in the spinal transmission and processing of noxious inputs that facilitate nociception.

In addition, a previous study in mice demonstrated that local IL-17 concentration increased significantly over time in methylated bovine serum albumin (mBSA)-injected knee joints, an intra-knee injection of IL-17 significantly decreased mechanical threshold, and co-treatment with mBSA and an IL-17 antibody significantly increased mechanical threshold [23].

Additionally, intra-plantar IL-17 induced significant mechanical allodynia and thermal hyperalgesia in mice [13; 19], IL-17 levels increased in injured sciatic nerves [15; 22], and an intra-sciatic nerve injection of recombinant IL-17 induced both mechanical allodynia and thermal hyperalgesia [13]. These data suggest that peripheral IL-17 plays roles in both inflammatory and neuropathic pain and substantiate that IL-17 is an important proinflammatory cytokine in both inflammatory and neuropathic pain.

4.3. IL-17 antiserum decreases spinal NR1 phosphorylation to inhibit pain

It is known that IL-17RA mediates the biological functions of IL-17. Our double immunofluorescence labeling shows that IL-17RA and NR1 co-localize in spinal neurons. IL-17RA has also been shown to be expressed in neurons after *in vivo* hypoxic stress [35]. Our previous study with Fos immunostaining demonstrated that NR1-immunoreactive neurons are activated during inflammation-induced pain [43], suggesting that NMDAR-containing neurons might be nociceptive. NMDAR involvement in the transmission of noxious messages in the spinal cord has been confirmed by electrophysiological and behavioral studies [4; 14; 26]. Thus the co-existence of IL-17RA and NR1 indicates that IL-17 might act on spinal NMDA receptor-containing nociceptive neurons to modulate NMDA receptors and so influence pain transmission.

Interestingly, IL-17 antiserum significantly inhibited inflammation-induced NR1 phosphorylation. Substantial evidence has established that hyperalgesia correlates with enhanced NR1 phosphorylation in the rat spinal cord [3; 7; 34] and that blockage of NR1 phosphorylation significantly reverses pain [7; 27]. Since NR1 phosphorylation plays a critical role in the transmission of noxious inputs in the spinal cord, it follows that IL-17 antiserum-produced inhibition of NR1 phosphorylation is associated with attenuation of inflammatory hyperalgesia.

Moreover, inhibition of NR1 phosphorylation by IL-17 antiserum also indicates that up-regulated IL-17 enhances NR1 phosphorylation in the spinal cord. This is substantiated by the fact that i.t. IL-17 significantly increased p-NR1 levels in the spinal cord and decreased PWL. The data show that IL-17 enhancement of NR1 phosphorylation may contribute to hyperalgesia.

Regarding mechanisms by which IL-17 enhances NR1 phosphorylation, IL-17 might act directly on NMDAR-containing neurons as suggested above. It has been demonstrated that protein kinase C (PKC) is involved in NR1 phosphorylation on serine 896 in the spinal cord in capsaicin-injected rats [46]. IL-17F might activate PKC in pulmonary microvascular endothelial cells [40]. Possible IL-17 activation of PKC in neurons warrants further investigation.

4.4. IL-17 antiserum decreases and IL-17 increases IL-17RA

In the present study, CFA-induced inflammatory pain also up-regulated IL-17RA in the spinal cord. Our *in situ* hybridization data demonstrate that IL-17RA mRNA is expressed in the same region. The real-time PCR data showed that IL-17RA mRNA was not up-regulated in the spinal dorsal horn during CFA-induced pain. Previous studies demonstrated that IL-17 commonly promotes gene expression by enhancing mRNA stability [10; 12]. This suggests that IL-17RA up-regulation may be accounted for by enhanced IL-17RA mRNA stability and protein translation.

Further, the up-regulation of IL-17RA was inhibited by IL-17 antiserum. Since IL-17 antiserum significantly attenuated CFA-induced hyperalgesia, the data suggests that IL-17 antibodies might alleviate pain by decreasing the IL-17RA that promotes transmission of

noxious messages in the spinal cord. In support of this, i.t. IL-17 significantly up-regulated IL-17RA in the spinal cord and decreased PWL; this was prevented by IL-17 antibodies.

In conclusion, the present study demonstrates that CFA-inflammation induces significant hyperalgesia accompanied by up-regulation of IL-17, IL-17RA, and P-NR1 in the spinal cord. An IL-17 antibody attenuates inflammatory hyperalgesia and suppresses IL-17RA and P-NR1. This suggests that spinal IL-17, produced by astrocytes, enhances NR1 phosphorylation to facilitate persistent inflammatory pain.

Supplementary Material

Refer to Web version on PubMed Central for supplementary material.

Acknowledgments

References

1. Almolda B, Costa M, Montoya M, Gonzalez B, Castellano B. Increase in Th17 and Treg lymphocytes and decrease of IL22 correlate with the recovery phase of acute EAE in rat. PLoS ONE. 2011; 6(11)

2. Costigan M, Moss A, Latremoliere A, Johnston C, Verma-Gandhu M, Herbert TA, Barrett L, Brenner GJ, Vardeh D, Woolf CJ, Fitzgerald M. T-Cell Infiltration and Signaling in the Adult Dorsal Spinal Cord Is a Major Contributor to Neuropathic Pain-Like Hypersensitivity. J Neurosci. 2009; 29:14415–14422. [PubMed: 19923276]

3. Daulhac L, Maffre V, Mallet C, Etienne M, Privat A-M, Kowalski-Chauvel A, Seva C, Fialip J, Eschalier A. Phosphorylation of spinal N-methyl-d-aspartate receptor NR1 subunits by extracellular signal-regulated kinase in dorsal horn neurons and microglia contributes to diabetes-induced painful neuropathy. Eur J Pain. 2011; 15:169.e161–169.e112. [PubMed: 20594879]

4. Dickenson AH, Sullivan AF. Differential effects of excitatory amino acid antagonists on dorsal horn nociceptive neurones in the rat. Brain Res. 1990; 506:31–39. [PubMed: 1967963]

5. Fossiez F, Djossou O, Chomarat P, Flores-Romo L, Ait-Yahia S, Maat C, Pin JJ, Garrone P, Garcia E, Saeland S, Blanchard D, Gaillard C, Das Mahapatra B, Rouvier E, Golstein P, Banchereau J, Lebecque S. T cell interleukin-17 induces stromal cells to produce proinflammatory and hematopoietic cytokines. J Exp Med. 1996; 183:2593–2603. [PubMed: 8676080]

6. Gaffen, SL.; Kramer, JM.; Yu, JJ.; Shen, F. The IL-17 Cytokine Family. In: Gerald, L., editor. Vitamins & Hormones. Vol. 74. Academic Press; 2006. p. 255-282.

7. Gao X, Kim HK, Chung JM, Chung K. Enhancement of NMDA receptor phosphorylation of the spinal dorsal horn and nucleus gracilis neurons in neuropathic rats. Pain. 2005; 116:62–72. [PubMed: 15936881]

8. Guo W, Wang H, Watanabe M, Shimizu K, Zou S, LaGraize SC, Wei F, Dubner R, Ren K. Glial-cytokine-neuronal interactions underlying the mechanisms of persistent pain. J Neurosci. 2007; 27:6006–6018. [PubMed: 17537972]

9. Hargreaves K, Dubner R, Brown F, Flores C, Joris J. A new and sensitive method for measuring thermal nociception in cutaneous hyperalgesia. Pain. 1988; 32:77–88. [PubMed: 3340425]

10. Hartupee J, Liu C, Novotny M, Li X, Hamilton T. IL-17 Enhances Chemokine Gene Expression through mRNA Stabilization. J Immunol. 2007; 179:4135–4141. [PubMed: 17785852]

11. Hemdan NY, Birkenmeier G, Wichmann G, Abu El-Saad AM, Krieger T, Conrad K, Sack U. Interleukin-17-producing T helper cells in autoimmunity. Autoimmun Rev. 2010; 9:785–792. [PubMed: 20647062]

12. Henness S, Johnson C, Ge Q, Armour CL, Hughes JM, Ammit AJ. IL-17 augments TNF-α–induced IL-6 expression in airway smooth muscle by enhancing mRNA stability. J Allergy Clin Immunol. 2004; 114:958–964. [PubMed: 15480342]

13. Kim CF, GM-T. Interleukin-17 contributes to neuroinflammation and neuropathic pain following peripheral nerve injury in mice. J Pain. 2011; 12:370–383. [PubMed: 20889388]

14. Kim HK, Kim JH, Gao X, Zhou JL, Lee I, Chung K, Chung JM. Analgesic effect of vitamin E is mediated by reducing central sensitization in neuropathic pain. Pain. 2006; 122:53–62. [PubMed: 16524661]

15. Kleinschnitz C, Hofstetter HH, Meuth SG, Braeuninger S, Sommer C, Stoll G. T cell infiltration after chronic constriction injury of mouse sciatic nerve is associated with interleukin-17 expression. Exp Neurol. 2006; 200:480–485. [PubMed: 16674943]

16. Li A, Zhang Y, Lao L, Xin J, Ren K, Berman BM, Zhang R-X. Serotonin Receptor 2A/C is Involved in Electroacupuncture Inhibition of Pain in an Osteoarthritis Rat Model. eCAM. 201110.1093/ecam/neq016:neq016

17. Li GZ, Zhong D, Yang LM, Sun B, Zhong ZH, Yin YH, Cheng J, Yan BB, Li HL. Expression of interleukin-17 in ischemic brain tissue. Scand J Immunol. 2005; 62:481–486. [PubMed: 16305645]

18. Lubberts E. Th17 cytokines and arthritis. Semin Immunopathol. 2010; 32:43–53. [PubMed: 20127485]

19. McNamee KE, Alzabin S, Hughes JP, Anand P, Feldmann M, Williams RO, Inglis JJ. IL-17 induces hyperalgesia via TNF-dependent neutrophil infiltration. Pain. 2011; 152:1838–45. [PubMed: 21507574]

20. Milligan ED, Twining C, Chacur M, Biedenkapp J, O'Connor K, Poole S, Tracey K, Martin D, Maier SF, Watkins LR. Spinal glia and proinflammatory cytokines mediate mirror-image neuropathic pain in rats. J Neurosci. 2003; 23:1026–1040. [PubMed: 12574433]

21. Murphy AC, Lalor SJ, Lynch MA, Mills KH. Infiltration of Th1 and Th17 cells and activation of microglia in the CNS during the course of experimental autoimmune encephalomyelitis. Brain Behav Immun. 2010; 24:641–651. [PubMed: 20138983]

22. Noma N, Khan J, Chen IF, Markman S, Benoliel R, Hadlaq E, Imamura Y, Eliav E. Interleukin-17 levels in rat models of nerve damage and neuropathic pain. Neurosci Lett. 2011; 493:86–91. [PubMed: 21316418]

23. Pinto LG, Cunha TM, Vieira SM, Lemos HP, Verri WA Jr, Cunha FQ, Ferreira SH. IL-17 mediates articular hypernociception in antigen-induced arthritis in mice. Pain. 2010; 148:247–256. [PubMed: 19969421]

24. Raghavendra V, Tanga F, DeLeo JA. Inhibition of microglial activation attenuates the development but not existing hypersensitivity in a rat model of neuropathy. J Pharmacol Exp Ther. 2003; 306:624–630. [PubMed: 12734393]

25. Raghavendra V, Tanga FY, DeLeo JA. Complete Freunds adjuvant-induced peripheral inflammation evokes glial activation and proinflammatory cytokine expression in the CNS. Eur J Neurosci. 2004; 20:467–473. [PubMed: 15233755]

26. Ren K, Hylden JLK, Williams GM, Ruda MA, Dubner R. The effects of a noncompetitiveNMDA receptor antagonist, MK-801, on behavioral hyperalgesia and dorsal horn neuronal activity in rats with unilateral inflammation. Pain. 1992; 50:331–344. [PubMed: 1454389]

27. Roh DH, Seo HS, Yoon SY, Song S, Han HJ, Beitz AJ, Lee JH. Activation of spinal alpha-2 adrenoceptors, but not mu-opioid receptors, reduces the intrathecal Nmethyl-D-aspartate-induced increase in spinal NR1 subunit phosphorylation and nociceptive behaviors in the rat. Anesth Analg. 2010; 110:622–629. [PubMed: 20007733]

28. Samad TA, Moore KA, Sapirstein A, Billet S, Allchorne A, Poole S, Bonventre JV, Woolf CJ. Interleukin-1beta-mediated induction of Cox-2 in the CNS contributes to inflammatory pain hypersensitivity. Nature. 2001; 410:471–475. [PubMed: 11260714]

29. Schulz SM, Kohler G, Holscher C, Iwakura Y, Alber G. IL-17 is produced by Th17, gammadelta T cells and other CD4- lymphocytes during infection with Salmonella enterica serovar Enteritidis and has a mild effect in bacterial clearance. Int Immunol. 2008; 20:1129–1138. [PubMed: 18599501]

30. Singh TP, Huettner B, Koefeler H, Mayer G, Bambach I, Wallbrecht K, Schön MP, Wolf P. Platelet-Activating Factor Blockade Inhibits the T-Helper Type 17 Cell Pathway and Suppresses Psoriasis-Like Skin Disease in K5. hTGF-[beta]1 Transgenic Mice. Am J Pathol. 2011; 178:699–708. [PubMed: 21281802]

31. Sweitzer S, Martin D, DeLeo JA. Intrathecal interleukin-1 receptor antagonist in combination with soluble tumor necrosis factor receptor exhibits an anti-allodynic action in a rat model of neuropathic pain. Neuroscience. 2001; 103:529–539. [PubMed: 11246166]

32. Sweitzer SM, Colburn RW, Rutkowski M, DeLeo JA. Acute peripheral inflammation induces moderate glial activation and spinal IL-1beta expression that correlates with pain behavior in the rat. Brain Res. 1999; 829:209–221. [PubMed: 10350552]

33. Tzartos JS, Friese MA, Craner MJ, Palace J, Newcombe J, Esiri MM, Fugger L. Interleukin-17 production in central nervous system-infiltrating T cells and glial cells is associated with active disease in multiple sclerosis. Am J Pathol. 2008; 172:146–155. [PubMed: 18156204]

34. Ultenius C, Linderoth B, Meyerson BA, Wallin J. Spinal NMDA receptor phosphorylation correlates with the presence of neuropathic signs following peripheral nerve injury in the rat. Neurosci Lett. 2006; 399:85–90. [PubMed: 16469445]

35. Wang DD, Zhao YF, Wang GY, Sun B, Kong QF, Zhao K, Zhang Y, Wang JH, Liu YM, Mu LL, Wang DS, Li HL. IL-17 potentiates neuronal injury induced by oxygen-glucose deprivation and affects neuronal IL-17 receptor expression. J Neuroimmunol. 2009; 212:17–25. [PubMed: 19457561]

36. Wang F, Flanagan J, Su N, Wang L-C, Bui S, Nielson A, Wu X, Vo H-T, Ma X-J, Luo Y. RNAscope: A Novel in Situ RNA Analysis Platform for Formalin-Fixed, Paraffin-Embedded Tissues. J Mol Diagn. 2012; 14:22–29. [PubMed: 22166544]

37. Watkins LR, Martin D, Ulrich P, Tracey KJ, Maier SF. Evidence for the involvement of spinal cord glia in subcutaneous formalin induced hyperalgesia in the rat. Pain. 1997; 71:225–235. [PubMed: 9231865]

38. Watkins LR, Milligan ED, Maier SF. Glial proinflammatory cytokines mediate exaggerated pain states: implications for clinical pain. Adv Exp Med Biol. 2003; 521:1–21. [PubMed: 12617561]

39. Yao Z, Fanslow WC, Seldin MF, Rousseau AM, Painter SL, Comeau MR, Cohen JI, Spriggs MK. Herpesvirus Saimiri encodes a new cytokine, IL-17, which binds to a novel cytokine receptor. Immunity. 1995; 3:811–821. [PubMed: 8777726]

40. You, Q-h; Sun, G-y; Wang, N.; Shen, J-l; Wang, Y. Interleukin-17F-Induced Pulmonary Microvascular Endothelial Monolayer Hyperpermeability Via the Protein Kinase C Pathway. J Surg Res. 2010; 162:110–121. [PubMed: 19577259]

41. Zhang R-X, Lao L, Wang L, Liu B, Wang X, Ren K, Berman BM. Involvement of opioid receptors in electroacupuncture-produced anti-hyperalgesia in rats with peripheral inflammation. Brain Res. 2004; 1020:12–17. [PubMed: 15312782]

42. Zhang R-X, Li A, Liu B, Wang L, Ren K, Zhang H, Berman BM, Lao L. IL-1ra alleviates inflammatory hyperalgesia through preventing phosphorylation of NMDA receptor NR-1 subunit in rats. Pain. 2008; 135:232–239. [PubMed: 17689191]

43. Zhang R-X, Wang H, Ruda M, Iadarola MJ, Qiao JT. c-Fos expression in NMDA receptor-contained neurons in spinal cord in a rat model of inflammation: a double immunocytochemical study. Brain Res. 1998; 795:282–286. [PubMed: 9622652]

44. Zhang X, Wu J, Lei Y, Fang L, Willis WD. Protein phosphatase modulates the phosphorylation of spinal cord NMDA receptors in rats following intradermal injection of capsaicin. Mol Brain Res. 2005; 138:264–272. [PubMed: 15919130]

45. Zou X, Lin Q, Willis WD. Enhanced phosphorylation of NMDA receptor 1 subunits in spinal cord dorsal horn and spinothalamic tract neurons after intradermal injection of capsaicin in rats. J Neurosci. 2000; 20:6989–6997. [PubMed: 10995844]

46. Zou X, Lin Q, Willis WD. Effect of protein kinase C blockade on phosphorylation of NR1 in dorsal horn and spinothalamic tract cells caused by intradermal capsaicin injection in rats. Brain Res. 2004; 1020:95–105. [PubMed: 15312791]
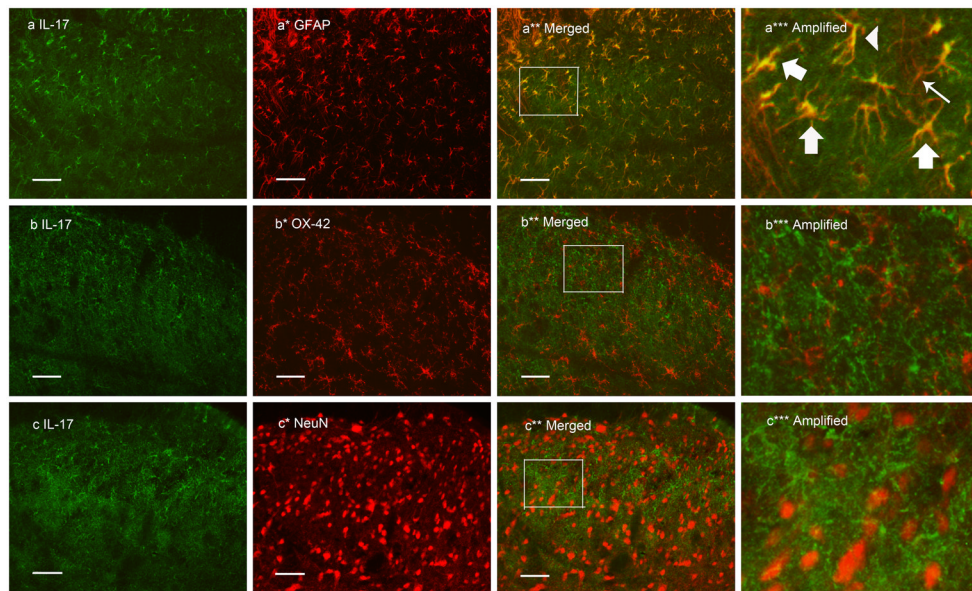
Fig. 1.
Photomicrographs showing IL-17 expression and co-localization of IL-17 and GFAP in ipsilateral lumbar spinal superficial laminae 24 h after CFA injection into one hind paw. Sections were double labeled with anti-IL-17 (green) and anti-GFAP, anti-OX-42, or anti-NeuN (red). The first column (a–c) is IL-17 immunostaining; the second column (a*–c*) is immunostaining of the astrocyte marker GFAP, microglia marker OX-42, and neuron marker NeuN. The third column (a**–c**) shows the merged graphs. The fourth column (a***–c***) shows images enlarged from the rectangles in a**–c**. The thin arrow (a***) points to a GFAP-singly labeled, non-activated cell. Yellow cells demonstrate GFAP and IL-17 double labeling, indicating that IL-17 is localized in astrocytes; thick arrows point to activated astrocytes that produce IL-17, and the arrow head points to a non-activated astrocyte that produces IL-17. Scale bars represent 50 µm.
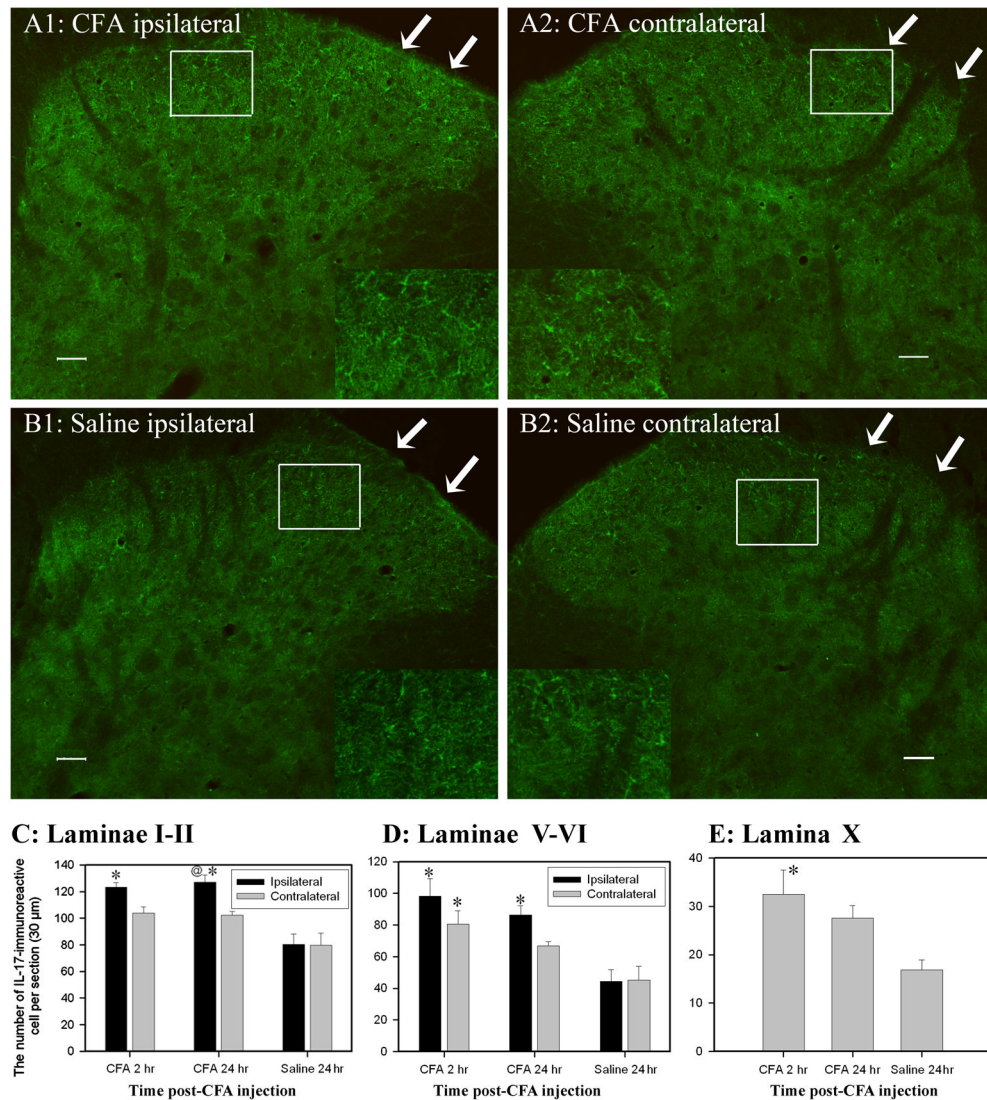
Fig. 2.
Values of IL-17 immunoreactive astrocytes in the spinal cord (Mean ± SEM). **A/B:**
Representative photographs showing IL-17 immunoreactive cells in superficial laminae of
the spinal cord 24 h after CFA (A1, A2) or saline (B1, B2) injection. Note that CFA
injection induced more IL-17 than did saline injection. Arrows point to superficial laminae.
C: The number of IL-17-immunoreactive astrocytes was increased in laminae I–II 2 and 24
h post-CFA compared to that of contralateral laminae and to that in saline-injected rats. **D:**
IL-17 also was significantly increased in both ipsilateral and contralateral spinal laminae V–
VI 2 h, and in ipsilateral laminae V–VI 24 h, post-CFA. **E:** IL-17 was significantly elevated
in lamina X 2 h post-CFA compared to saline control. * P<0.05 vs. saline-injected
rats; [@]P<0.05 vs. contralateral laminae. Scale bars represent 50 μm.
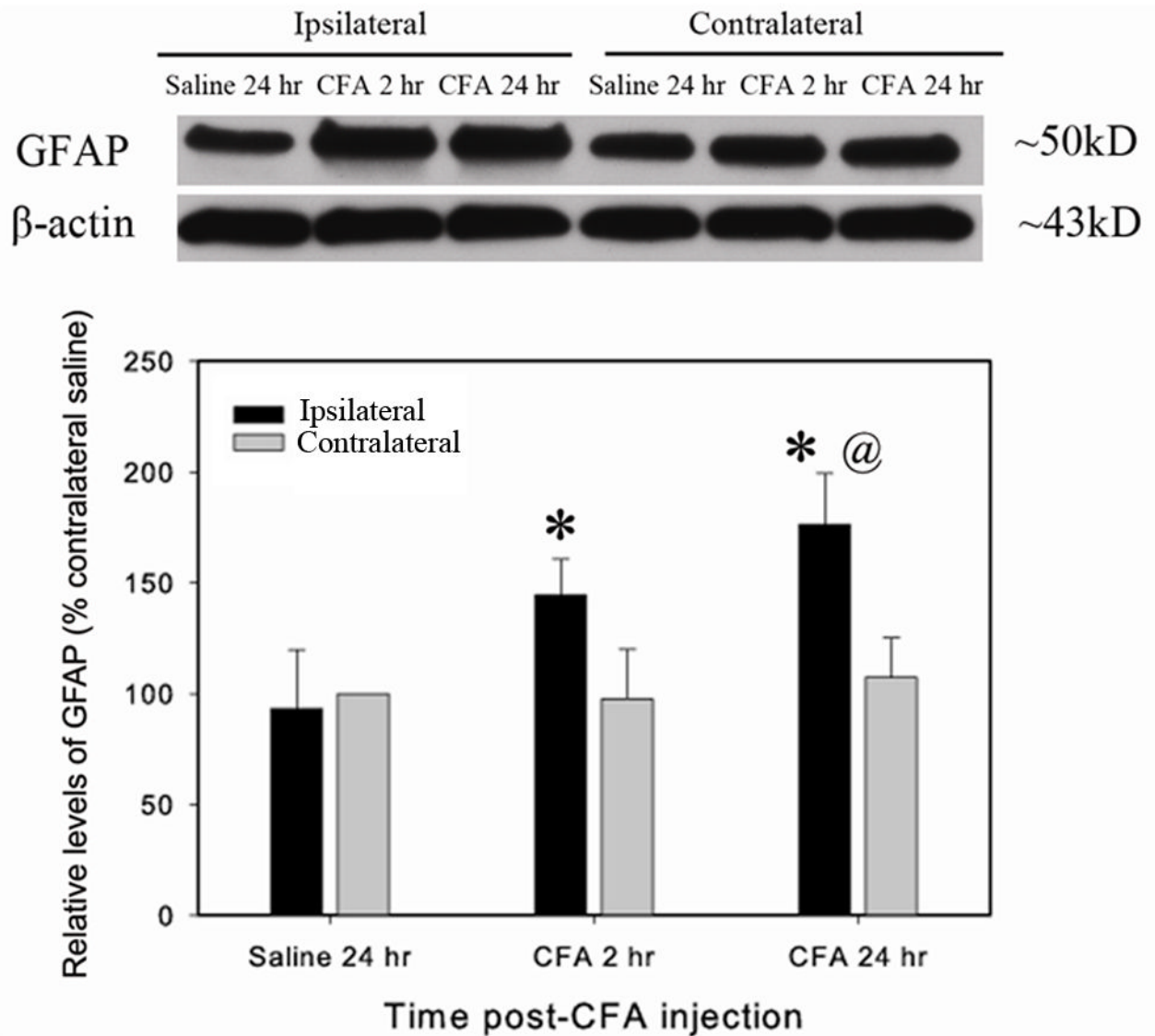
Fig. 3.
Spinal GFAP expression during CFA-induced peripheral inflammation. CFA was subcutaneously injected into the hind paw. **A.** A representative GFAP western blot. Note that GFAP was significantly upregulated in the ipsilateral but not the contralateral spinal dorsal horn. **B.** Quantification of relative levels of GFAP. The values were normalized using saline-injected rats as control (100%). CFA induced a significant increase 2–24 h post CFA-injection compared to saline-injected control. *$P<0.05$ vs. saline-injected control and [@]$P<0.05$ vs. contralateral side (n=4 per group).
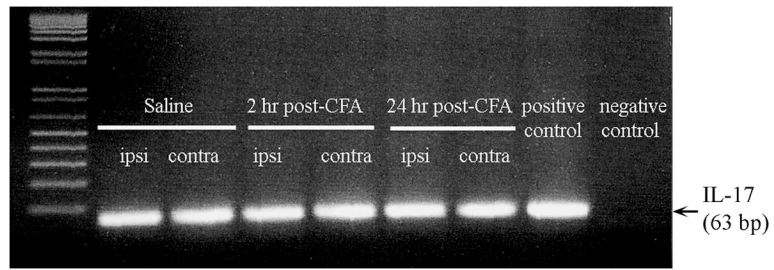
Fig. 4.
Expression of IL-17 in the spinal dorsal horn (n=2–3/group). The bands represent the total PCR product after 50 cycles of amplification.
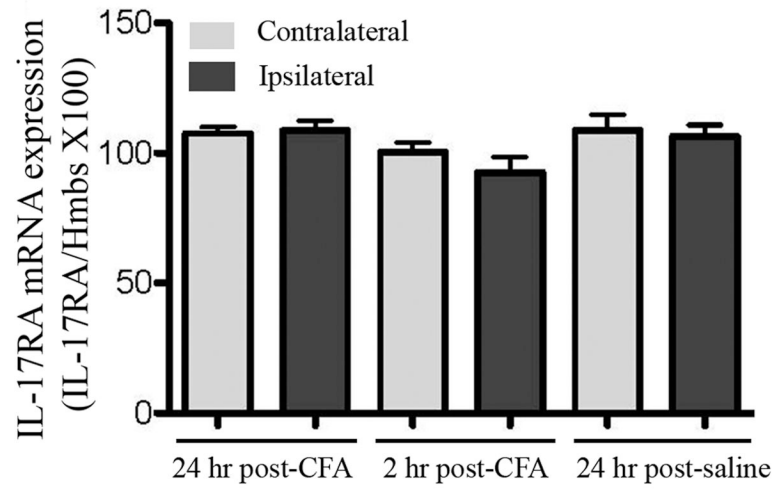
Fig. 5.
Expression of the IL-17RA mRNA in the spinal dorsal horn (n=6/group). Expressions are shown relative to the expression of Hmbs, an internal control. Values are expressed as means ± SE. There were no significant changes among the groups.
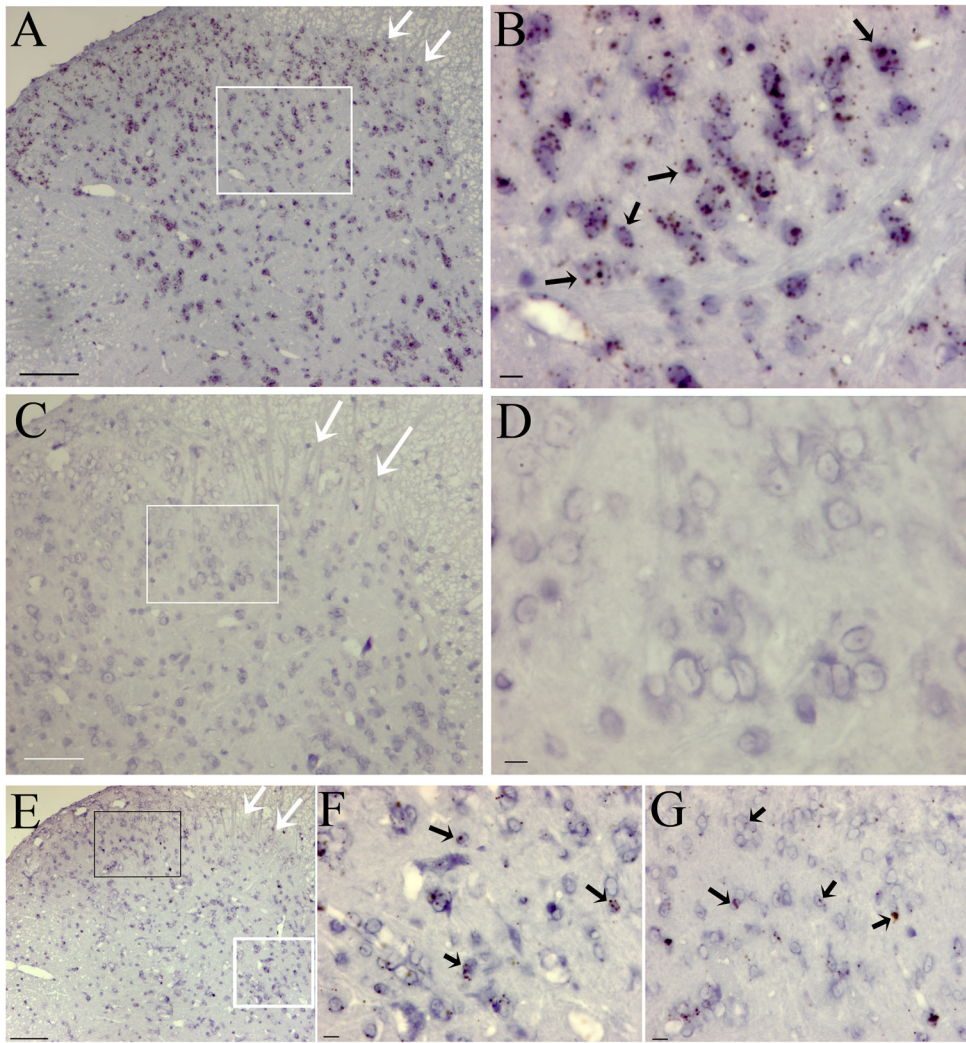
Fig. 6.
Representative microphotographs of *in situ* hybridization staining of the spinal cord. **A:** Positive staining of spinal cord using RNAscope Positive Control Probe, POLR2A (cat# 312481). **B:** Magnification of white box in A; arrows point to cells containing brown, punctate dots in the cytoplasm. **C:** Negative staining of spinal cord using RNAscope Negative Control Probe, DapB (cat# 310043). **D:** Magnification of white box in C; note that there are no brown, punctate dots in the cytoplasm. **E:** *In situ* hybridization staining of spinal cord with IL-17RA probe. **F & G:** Respective magnifications of white and black boxes in E; arrows point to cells containing brown, punctate dots in the cytoplasm, which shows that IL-17RA mRNA was in those cells. The counterstaining demonstrates that the IL-17RA mRNA-positive cells are oval and round at ~ 7μm. White arrows point to superficial laminae of the dorsal horn in A, C, and E. Scale bars are 100 μm in A, C, and E and 10 μm in B, D, F, and G.
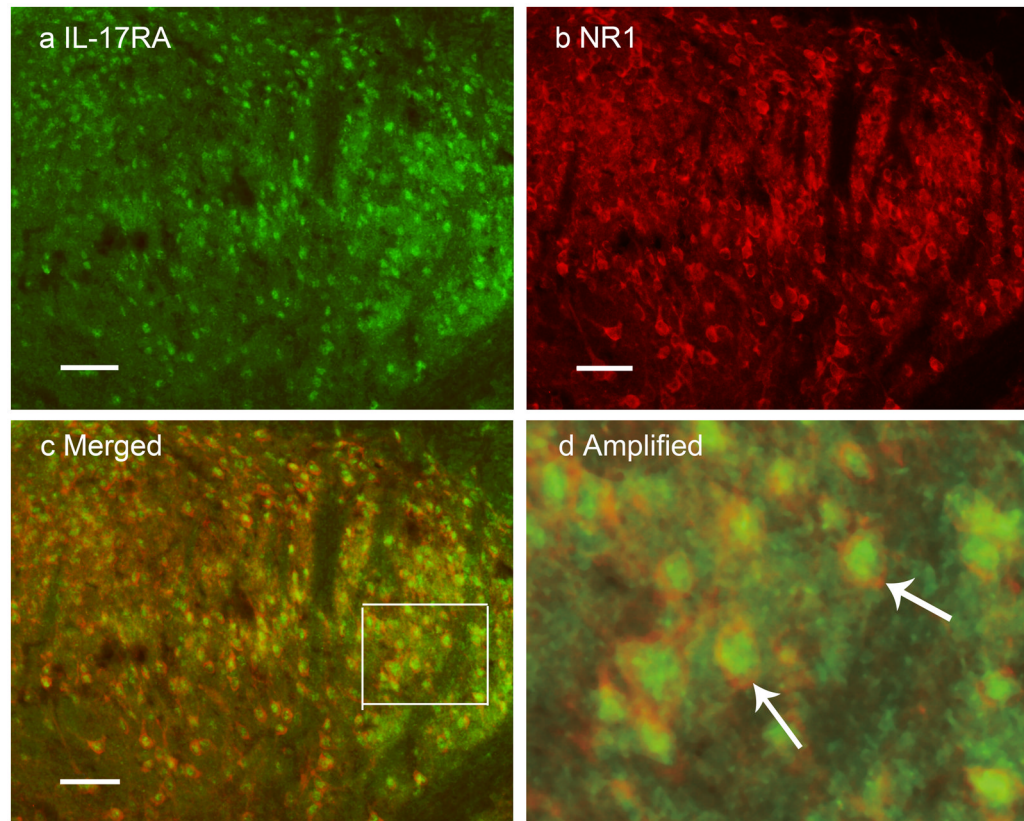
Fig. 7.
Micrographs showing co-localization of NR1 and IL-17RA in lumbar spinal dorsal horn neurons. Sections were double labeled with anti-IL-17RA (green) and anti-NR1 (red). **a:** IL-17RA-immunoreactive neurons in laminae I–II. **b:** NR1-immunoreactive neurons in laminae I–II. **c**: Merged graphs of a and b. d: Magnification of box in c. Arrows indicate double-labeled NR1/IL-17RA neurons (yellow); scale bars represent 50 μm.
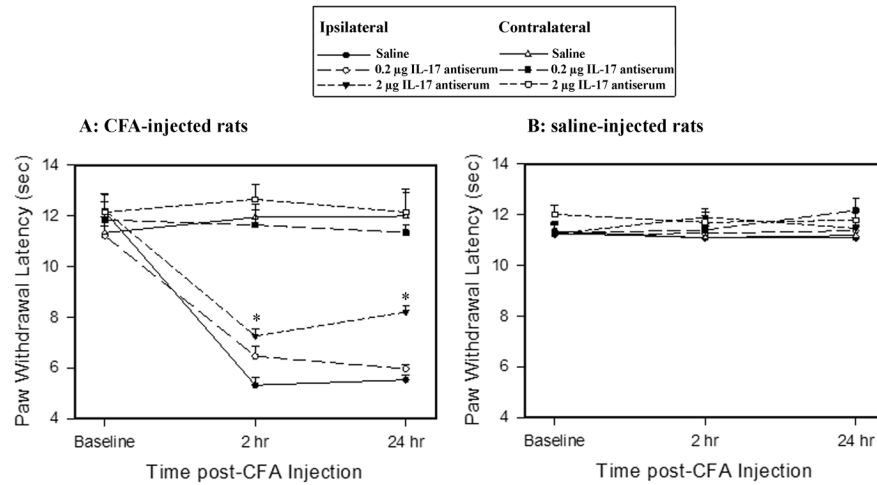
Fig. 8.
Effects of IL-17 antiserum on PWL in CFA- (A) and saline-injected (B) rats (n = 7/group). IL-17 antiserum at 0.2 and 2 μg/rat (10 μl) was given (i.t.) three times: 24 h before CFA but after baseline measurement, and 2 h prior to each of two hyperalgesia tests. **A:** IL-17 antiserum at 2 μg/rat (i.t.) significantly increased ipsilateral PWL compared to vehicle control but had no effect on contralateral PWL. *P<0.05 vs. saline-injected control. **B:** IL-17 antiserum did not alter the PWL in saline-injected rats.
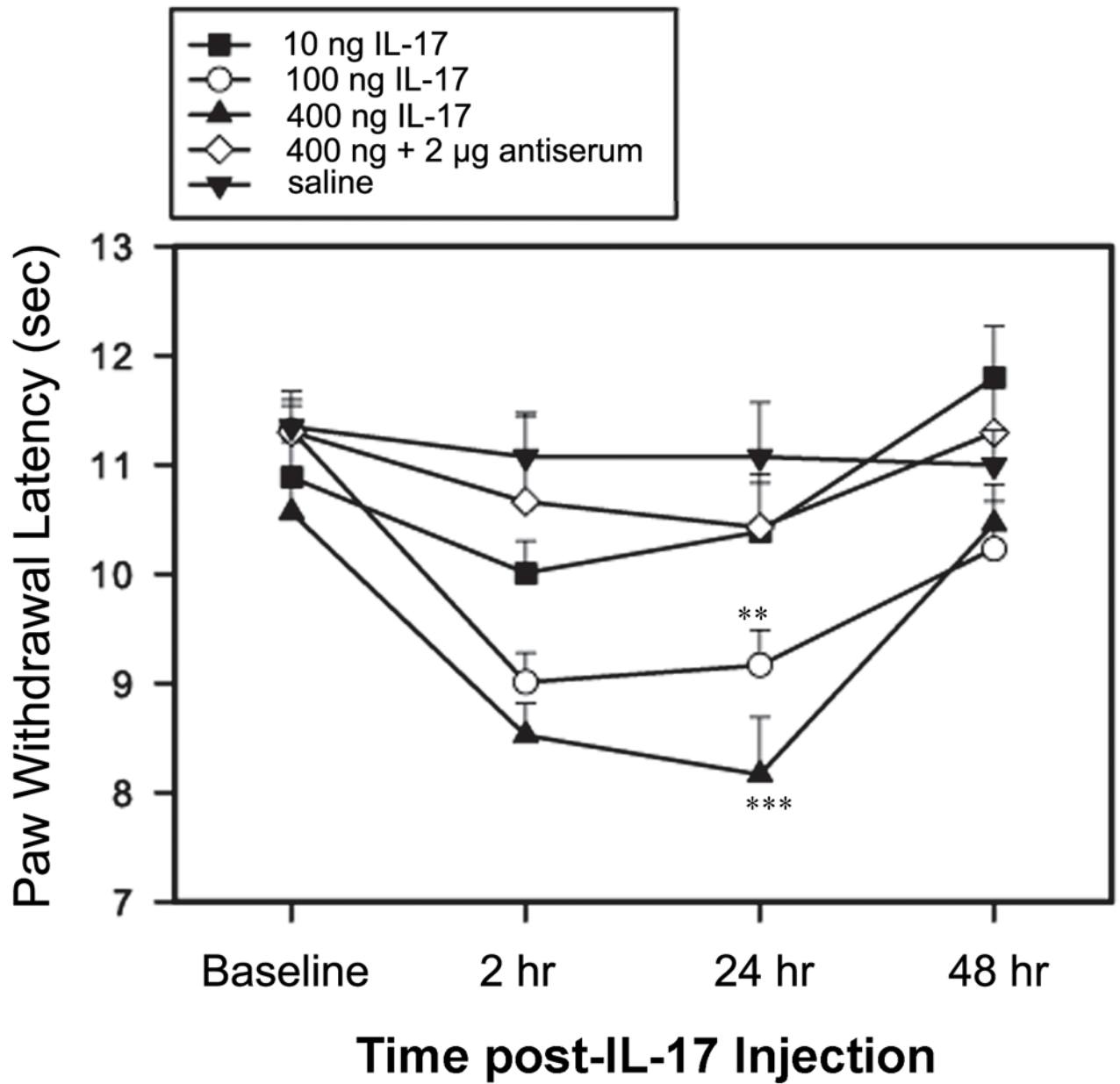
Fig. 9.
Effect of IL-17 on left PWL in naive rats (n = 7 per group). IL- 17 at 100–400 ng/rat, given (i.t.) once after baseline measurement, significantly decreased PWL. IL-17 antiserum at 2 µg/rat prevented PWL decrease. **P<0.01 and ***P<0.001 vs. saline control.
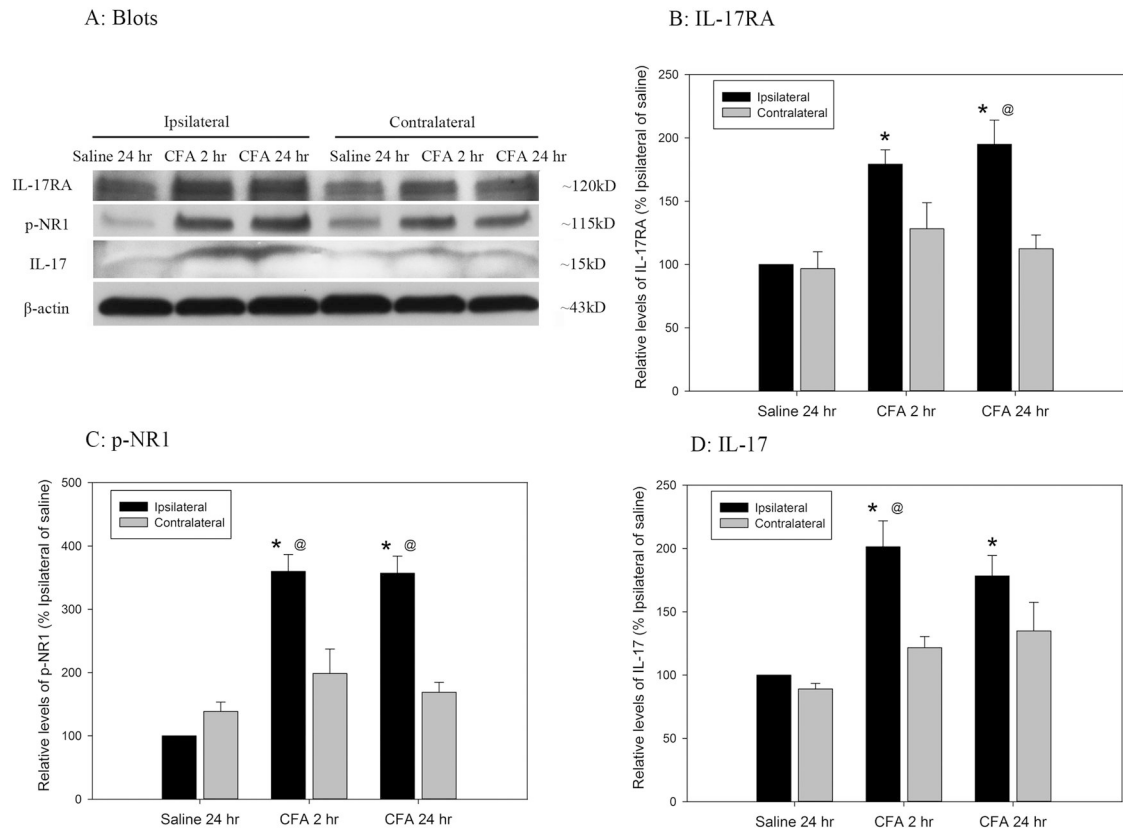
Fig. 10.
Time course of IL-17RA, p-NR1, and IL-17 expression in the spinal dorsal horn after inflammation. **A:** Representative western blots showing that IL-17RA, p-NR1, and IL-17 expression is greater in CFA- than in saline-injected rata, and ipsilaterally than contralaterally. **B–D:** Quantification of relative levels of IL17RA (B), p-NR1 (C), and IL-17 (D). IL-17RA, p-NR1, and IL-17 values were normalized using saline-injected rats as a control (100%). CFA induced a significant increase in IL-17RA, p-NR1, and IL-17 2–24 h post CFA-injection compared to saline-injected control (CFA vs. saline-injection). *P<0.05 vs. saline-injected control and @P<0.05 vs. contralateral section (n=4 per group).
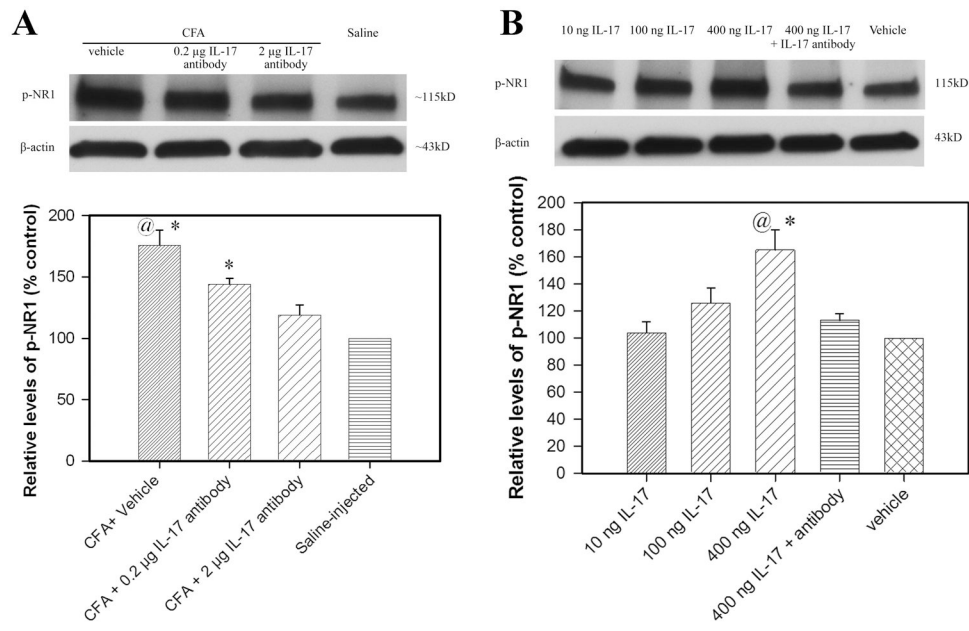
Fig. 11.
A: Effects of IL-17 antibody on spinal cord NR1 phosphorylation (n= 4 per group). The values of NR1 phosphorylation in saline-injected rats were arbitrarily set at 100%. Each bar is expressed as a percentage of that in the saline-injected rats. CFA induced significant NR1 phosphorylation compared to saline-injected control (CFA + vehicle vs. saline-injection). IL-17 antibody at 2 μg/rat (i.t.) significantly inhibited spinal cord NR1 phosphorylation compared to vehicle control. *P<0.05 vs. saline-injected control and [@]P<0.05 vs. CFA + 2 μg IL-17 antibody. **B:** Effects of IL-17 on spinal cord NR1 phosphorylation in naive rats. IL-17 dosage-dependently induced NR1 phosphorylation compared to saline-injected control. IL-17 antibody at 2 μg/rat (i.t.) significantly inhibited spinal cord NR1 phosphorylation compared to vehicle control. *P<0.05 vs. vehicle and [@]P<0.05 vs. IL-17 + 2 μg IL-17 antibody.
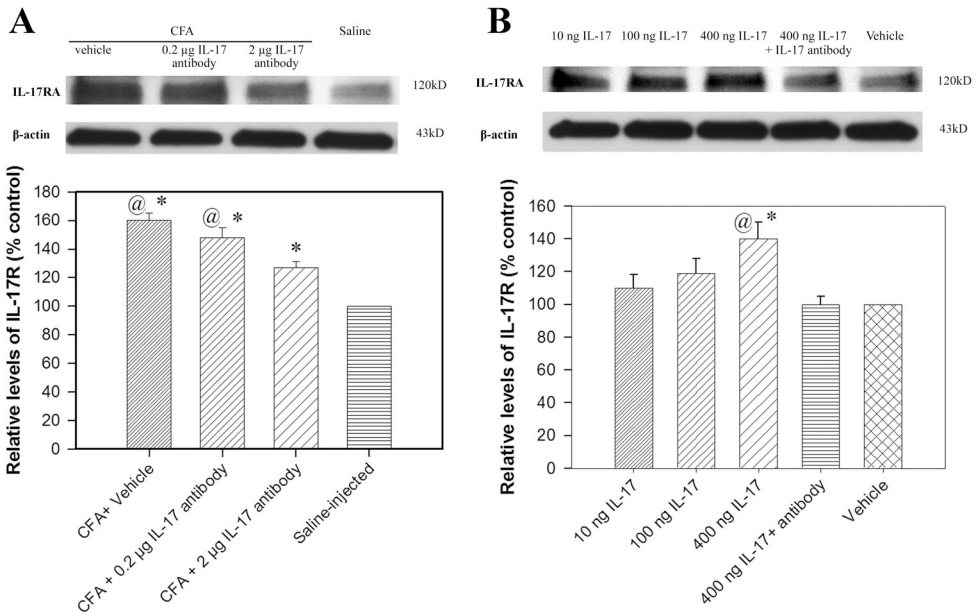
Fig. 12.
A: Effects of IL-17 antibody on spinal cord IL-17RA (n= 4 per group). The values of IL-17RA in saline-injected rats were arbitrarily set at 100%. Each bar is expressed as a percentage of that in the saline-injected rats. CFA induced a significant increase in IL-17RA compared to saline-injected control (CFA + vehicle vs. saline-injection). IL-17 antibody at 2 μg/rat (i.t.) significantly decreased spinal cord IL-17RA compared to vehicle control. *P<0.05 vs. saline-injected control and [@]P<0.05 vs. CFA + 2 μg IL-17 antibody. **B:** Effects of IL-17 on spinal cord IL-17RA in naive rats. IL-17 dosage-dependently increased IL-17RA compared to saline-injected control. IL-17 antibody at 2 μg/rat (i.t.) significantly inhibited spinal cord IL-17RA compared to vehicle control. *P<0.05 vs. vehicle and [@]P<0.05 vs. IL-17 + 2 μg IL-17 antibody.